Penerbit Akademia Baru

CFD Letters

Journal homepage: www.akademiabaru.com/cfdl.html
ISSN: 2180-1363

Conjugate Natural Convection in a Partitioned Square Cavity Filled with Al_2O_3-Water Nanofluid Based on Experimental Correlations: a Lattice Boltzmann investigation

Open

Mokhtar Ferhi[1,2,*], Ridha Djebali[2] , Said Abboudi[3]

[1] National Superior School of Engineering of Tunis, University of Tunis, 5 Avenue Taha Hussein, 1008 Tunis, Tunisia
[2] Laboratory of Subatomic Physics, Nanosciences and Energetics, IPEST, University of Carthage, Tunisia
[3] ICB UMR 6303, CNRS, Université de Bourgogne Franche-Comté, UTBM Département COMM, F-90010, Belfort, France

ARTICLE INFO

Article history:
Received 3 December 2018
Received in revised form 23 February 2019
Accepted 28 February 2019
Available online 22 March 2019

Keywords:
Conjugate heat transfer, partitioned cavity Al_2O_3-nanofluids, experimental correlations, Lattice Boltzmann method.

ABSTRACT

In this paper a numerical investigation of conjugate natural convection inside a divided square cavity filled with Al_2O_3-water nanofluid is performed. The lattice Boltzmann method (LBM) is used to solve the governing equations. The nanofluid thermo-physical properties are selected based on literature experimental correlations. The grid independency was checked and the LBM code model was validated on two different cases for wide ranges of the present problem monitoring parameters. A good agreement is obtained by comparison with reported results in the literature. The study of the conjugate heat transfer and nanoliquid motion is, afterward, conducted for the ranges of nanoparticles volume fraction (%): $1 \leq \phi \leq 4$, temperature (°C): $20 \leq T \leq 40$, particle size (nm): $15 \leq d_p \leq 120$ and Rayleigh number: $10^3 \leq Ra \leq 10^6$. It will be shown firstly that, at room temperature, the viscosity and the thermal conductivity experimental correlations based models give results in strong deviation compared to theoretical ones. The effects of the aforementioned problem parameters on local and average heat transfer and velocity profiles are explored and discussed. Results show a heat transfer rise by increasing the temperature. However, for the Al_2O_3 nanoparticles size, the enhancement marked a maximum close to d_p=33nm in a concave behavior. The heat transfer and the fluid motion are dumped by increasing the volume fraction ϕ (%) and the nanoparticles size ($d_p \geq 35$nm) due to the reduced effective Ra* number.

1. Introduction

The Lattice Boltzmann Method (LBM), derived from the models of the lattice gas automata [1], has been developed as an alternative numerical scheme for solving the incompressible Navier-Stokes equations. In the last few years, this method has received exceptional attention. A rapid rise of the application of the LBM was noted in several fields, including physical, chemical, biological, and sciences for academic, research and engineering purpose. In this context the lattice Boltzmann

*Corresponding author.
E-mail address: moktar ferhi@gmail.com(Mokhtar Ferhi)

method (LBM) is used to predict moving solid particles in a fluid flow [2]. Recently, the LB method was also applied to simulate nanofluids successfully.

Recent advances in nanotechnology have allowed development of a new category of fluids termed nanofluids, a suspension containing small amounts of nanoparticles or carbon nanotubes with diameters below 100nm. An innovative technique to enhance heat transfer is by using nano-scale particles in the base fluid. Nano-scale particle added to fluids are called as nanofluid which is firstly utilized by Choi [3]. Until today, nanofluids are used by many researches [4].

nanofluids are used in various industrial processes such as Micro Electro Mechanical Systems (MEMS) [5], cooling of electronic elements [6-9], Cooling of thermal systems used in the automobile industry [10-12], cooling of nuclear system and Biomedicine Jordan *et al*., [13] and many other applications of nanofluids in heat transfer devices [14].

During the past decade, according to literature, the addition of nanoparticles has been noticed to cause the enhancement of convective heat transfer performance of a fluid. The theoretical models developed by Maxwell [15], Hamilton and Crosser [16], and Davis [17] corresponding to the thermal conductivity are used in the most cases. For the dynamic viscosity the most of researchers use the Brinkman model [18]. Several theoretical studies in the literature have reported to estimate the viscosity and thermal conductivity of nanofluids. Consequently, the impact of these physical parameters on the natural heat transfer and the behavior of the flow are studied by many researchers.

Jahanshahi *et al*., [19] investigated heat transfer enhancement in a square cavity subject to different side wall temperatures using water/SiO_2 nanofluid based on experimental measured conductivity. The Rayleigh number of base fluid, $Ra_f=10^5–10^7$ and the volume fraction of nanoparticle between 0 and 4%. The results show a considerable enhancement in heat transfer by increasing the concentration of nanoparticules in the base fluid at any Rayleigh number for the experimental thermal conductivity model. On the other hand, the results show a decrease in heat transfer for the theoretical thermal conductivity model (Hamilton and Crosser model).

Lai and Yang [20], analyzed the impacts of natural convection heat transfer in a square cavity loaded with Al_2O_3/water nanofluid. They have taken the nanoparticles size of 42 nm for the simulation. They found that the average Nusselt number increases with the increasing Rayleigh number and the addition of Al_2O_3 nanoparticles. They found a significant under-estimation of nanofluid viscosity by using theoretical models.

Kefayati [21], studied the natural convection in an open-ended enclosure that contains Cu-water nanofluid. The simulation is carried out for various ranges of parameters like Rayleigh number, the volume fraction of nanoparticles, and aspect ratio of the cavity. The results demonstrate that the decrease in aspect ratio and increase in Rayleigh number enhance the heat transfer rate. They found that the impact of nanoparticles was observed to be maximum when the aspect ratio is 2.

Selvan [22] investigated numerically the flow motion and heat transfer enhancement in a bottom heated lid-driven square cavity filled with nanofluids. They found that the heat transfer coefficient of nanofluids increases with increasing value of the nanoparticles concentration. The average Nusselt number is linear function of solid volume fraction.

Snoussi *et al.,* [23] investigated numerically the heat transfer enhancement for natural convection in a cubical enclosure filled with Al_2O_3/water and Ag/water nanofluids. Authors found that the heat transfer decreases with increasing the particle volume fraction, especially at high Rayleigh numbers. A similar trend in the increase of the Nusselt number with the Rayleigh number is also observed.

Sheikholeslami *et al.,* [24] investigated numerically free convection of nanofluid in annuli enclosure filled with water including various kinds of nanoparticles using the Lattice Boltzmann Method. The viscosity and the effective thermal conductivity of nanofluids are respectively simulated using Maxwell-Garnetts and Brinkman models. The rate of heat transfer enhances by adding nanoparticles, though the maximum rate of heat transfer is obtained when copper is selected as the nanoparticle. Authors found that as the aspect ratio decreases, the Nusselt number increases. Also, they observed a different behavior for Nu_h when the aspect ratio increases. The minimum value of Nu_h is obtained at the aspect ratio equal to 2.5, and the maximum value of it occurs at the aspect ratio equal to 1.5 whereas Nu_h shows an increasing trend with respect to the aspect ratio for Ra = 10^5, 10^6. The maximum value of enhancement is related to at the aspect ratio equal to 2.5 at Ra = 10^6, while for other Rayleigh numbers, it is obtained at the aspect ratio equal to 1.5.

Bararnia *et al.,* [25] studied the effects of inclination angle and Rayleigh number on free convection in a partitioned space filled with a nanofluid using theoretical correlations. Besides, Brinkman and Maxwell models are used for viscosity thermal conductivity respectively. They found that the vertical partition leads the highest heat transfer rate. The application of nanofluids leads to increase in the Nusselt number compared to the base fluid.

Zahan and Alim [26] investigated numerically a model regarding conjugate effect of fluid flow and heat transfer in a heat conducting vertical walled cavity filled with copper-water nanofluid. The governing equations of this model have been solved by using finite element method of Galerkin weighted residual approach. The study has been carried out for the Rayleigh number Ra =10^6 and for the solid volume fraction $0 \leq \varphi \leq 0.05$. Authors found that the heat transfer rate decrease by means of raising the convective heat transfer coefficient. It is also pragmatic that at a higher h_∞ the existence of the nanoparticles is more valuable. The position of the partition contributes to enhance the heat transfer rate when the divider gets closure to the cold wall. The influence of the flow circulation of the fluid is much higher with thin wall. The average Nuselt number decrease by increasing the wall thickness and he becomes constant for the highest values of the thickness parameter. In another study Zahan and Alim [27] analyzed the effect of Rayleigh number and thermal conductivity ratio on the hydrodynamic and thermal characteristic of flow. They found that the Rayleigh number have a significant effect of on the pattern of streamlines and isotherms in the cavity. The Nusselt number is an increasing function of Rayleigh number. It is found that the rate of heat transfer increases and the fluid moves with greater velocity when the value of Rayleigh number and conductivity ratio increase.

Recently, many experimental studies are available in the literature have been conducted in order to estimate the dynamic viscosity and thermal conductivity of nanofluid. Due to the underestimation of the theoretical models of the dynamic viscosity and thermal conductivity, a modern development of empirical correlations based on the experimental measurements has been performed.

He *et al.,* [28] studied natural convection in a square cavity filled with alumina-water nanofluid. They found that the heat transfer characteristics transform from conduction to convection as the Rayleigh number increases, the average Nusselt number is reduced with increasing volume fraction of nanoparticles, especially at high Rayleigh number. The flow and heat transfer characteristics of Al_2O_3-water nanofluid in a square cavity are demonstrated to be more sensitive to viscosity than to thermal conductivity.

Jalali and Abbassi [29] performed a numerical simulation based on experimental correlations in a square cavity heated from the bottom filled with a mixture of water and Al_2O_3 nanoparticles. They found that the heat transfer decrease with increasing the concentration of Al_2O_3 nanoparticles

in the base fluid. The heat transfer is strongly affected by increasing the size of Al_2O_3 nanoparticles. Besides, the enhancement of heat transfer is detected only when d_p exceed 20 nm.

Alawi *et al.,* [30] estimated the thermal conductivity and viscosity of various types of metallic oxides for nanoparticle concentrations ranging from 0 to 5% at temperatures of 300–320K and different nanoparticle shapes. They found that the effective thermal conductivity and thermal conductivity ratio of metallic oxide nanofluids increase with temperature and nanoparticles volume fraction but decreases when the nanoparticles size intensifies.

Etaig *et al.,* [31] proposed a new model predicting the viscosity of the nanofluids. They found that the theoretical models underestimate the viscosity at higher volume fractions. The effective viscosity increases with the increase of the volume fraction and decrease with temperature.

Nguyen *et al.,* [32] made an experimental investigation of Al_2O_3 nanofluids at high volume concentration. In his study the temperature presents an important factor for both pure fluid and nanofluid. The results showed that although both viscosities of water and Al_2O_3 nanofluid decrease as the temperature increases, the effective viscosity ratio of Al_2O_3 nanofluid decrease firstly and then increase as temperature increases. And the lowest viscosity of nanofluid was obtained at 43°C for 1vol%. The effect of temperature on the effective viscosity ratio of nanofluid is weaker than the particle concentration.

Khanafer and Vafai [33], According to literature, they developed a new correlation for the effective viscosity of water based Al_2O_3 nanofluid from curve fitting of the experimental data [32], [34-36]. In addition, these authors developed a new model corresponding to the thermal conductivity. The models are valid for Al_2O_3 nanofluids with temperatures between 20 and 70°C, nanoparticles diameters between 13 and 131 nm and concentrations of Al_2O_3 in the base fluid range between 1% and 9%. They conclude that the viscosity of nanoflluid plays a key role in predicting the heat transfer characteristics. Corcione [37] formulated a viscosity and thermal conductivity correlations from various experimental data of nanofluid. Their correlations are valid for a temperature range from 293 to 333 K, volume concentration range from 0.1% to 7.1% and a particle size ranging between 25 and 200 nm. He found that the effective thermal conductivity and the dynamic viscosity increases as the nanoparticles volume fraction and the temperature are increased, and the nanoparticles diameter is decreased. The effective viscosity is independent of temperature. Sekhar and Sharma [38] presented a regression equation including the effect of particle concentration, particle size and temperature of the base fluid. It is based on the experimental data [39-42] from the literature. They observed that the model was in a good agreement with the experimental data of different authors with a deviation of –10 to +18%. The correlation is valid in the range of 13 nm < d_p < 100 nm particle size, 20 °C < T_{nf} < 50 °C and 0.01% < ϕ < 4% volume concentration.

The aim of this numerical research is to study the performance of the nanofluid conjugate convective heat transfer in two-dimensional differentially heated cavity divided with an exchanger. The effect of several operating parameters such as solid volume fraction (ϕ), the Rayleigh number (Ra), the temperature (T), the diameter size (d_p), the dynamic viscosity and the thermal conductivity, on the heat transfer is studied. At ambient temperature, models for viscosity and thermal conductivity based on experimental measurements of water based Al_2O_3 nanofluids are used. Other models based on experimental measurements combining effects of temperature, concentration and nanoparticles sizes are also used to evaluate their effects on conjugate heat transfer and the dynamic of the flow inside the divider cavity.

2. Mathematical formulation

2.1. Problem statement

Figure 1 demonstrates a schema of the physical model for conjugate natural convection heat transfer in square cavity divided with an exchanger. The height and the width of the enclosure are given by H and W, respectively. The horizontal walls are adiabatic while the entire right wall was held at the isothermal cold temperature T_c and the cavity is heated with the hot temperature T_h from the left vertical wall. All the walls are rigid and no-slip BC is considered. Detailed of The non-dimensional boundary conditions is listed in Table 1. The divided cavity is filled with Al_2O3-water nanofluid.

a) It was assumed that the Al_2O_3 solid nanoparticles were always stable and suspended in water, means that there was no sedimentation or accumulation of nanoparticles.
b) The nanofluid is considered as a single-phase.
c) The Al_2O_3 solid nanoparticles have a spherical form

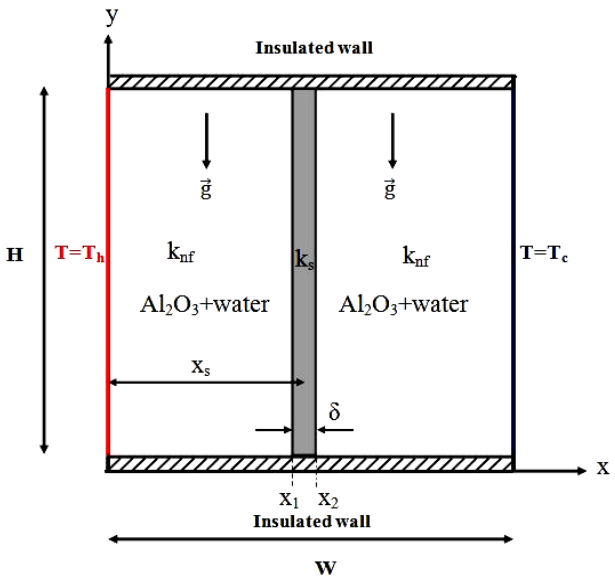

Fig. 1. Physical domain and coordinate system.

Steady and laminar flow is considered. The density variation in the nanofluid is approximated by the standard Boussinesq approximation. The viscous dissipation and Joule heating are neglected.

2.2. Governing equations

Considering the above mentioned assumptions, the governing equations of nanoliquid motion and heat transfer in dimensional form namely the Navier–Stokes coupled with the energy equations are given as follow:

Continuity equation

$$\frac{\partial u}{\partial x}+\frac{\partial v}{\partial y}=0 \tag{1}$$

Momentum equations

$$\rho_{nf}\left(\frac{\partial u}{\partial t}+u\frac{\partial u}{\partial x}+v\frac{\partial u}{\partial y}\right)=-\frac{\partial p^{*}}{\partial x}+\mu_{nf}\left(\frac{\partial^{2}u}{\partial x^{2}}+\frac{\partial^{2}u}{\partial y^{2}}\right) \tag{2}$$

$$\rho_{nf}\left(\frac{\partial v}{\partial t}+u\frac{\partial v}{\partial x}+v\frac{\partial v}{\partial y}\right)=-\frac{\partial p^{*}}{\partial y}+\mu_{nf}\left(\frac{\partial^{2}v}{\partial x^{2}}+\frac{\partial^{2}v}{\partial y^{2}}\right)+(\rho\beta)_{nf}\,g\left(T_{f}-T_{c}\right) \tag{3}$$

Energy equation for the fluid

$$\frac{\partial T_{f}}{\partial t}+u\frac{\partial T_{f}}{\partial x}+v\frac{\partial T_{f}}{\partial y}=\alpha_{nf}\left(\frac{\partial^{2}T_{f}}{\partial x^{2}}+\frac{\partial^{2}T_{f}}{\partial y^{2}}\right) \tag{4}$$

Energy equation for the solid

$$\frac{\partial^{2}T_{s}}{\partial x^{2}}+\frac{\partial^{2}T_{s}}{\partial y^{2}}=0 \tag{5}$$

The above equations are normalized using the following dimensionless variables:

$$X=\frac{x}{W},\ Y=\frac{y}{W},\ U=\frac{uW}{\alpha_{nf}},\ V=\frac{vW}{\alpha_{nf}},\ p=\frac{p^{*}W^{2}}{\rho_{nf}\alpha_{nf}^{2}},\ \theta=\frac{T-T_{c}}{T_{h}-T_{c}},\ Ra=\frac{g\beta\left(T_{h}-T_{c}\right)W^{3}}{\alpha_{f}\upsilon_{f}},\ \tau=\frac{t\alpha_{nf}}{W^{2}}$$

$$Pr=\frac{\upsilon_{f}}{\alpha_{f}}$$

The non-dimensionalized continuity, momentum and energy equations for nanofluid and solid body are expressed as:

$$\frac{\partial U}{\partial X}+\frac{\partial V}{\partial Y}=0 \tag{6}$$

$$\frac{\partial U}{\partial \tau}+U\frac{\partial U}{\partial X}+V\frac{\partial U}{\partial Y}=-\frac{\partial P}{\partial X}+Pr^{*}\left(\frac{\partial^{2}U}{\partial X^{2}}+\frac{\partial^{2}U}{\partial Y^{2}}\right) \tag{7}$$

$$\frac{\partial V}{\partial \tau}+U\frac{\partial V}{\partial X}+V\frac{\partial V}{\partial Y}=-\frac{\partial P}{\partial Y}+Pr^{*}\left(\frac{\partial^{2}V}{\partial X^{2}}+\frac{\partial^{2}V}{\partial Y^{2}}\right)+Ra^{*}\,Pr^{*}\,\theta \tag{8}$$

$$\frac{\partial \theta_{f}}{\partial \tau}+U\frac{\partial \theta_{f}}{\partial X}+V\frac{\partial \theta_{f}}{\partial Y}=\frac{\partial^{2}\theta_{f}}{\partial X^{2}}+\frac{\partial^{2}\theta_{f}}{\partial Y^{2}} \tag{9}$$

$$\frac{\partial^{2}\theta_{s}}{\partial X^{2}}+\frac{\partial^{2}\theta_{s}}{\partial Y^{2}}=0 \tag{10}$$

where Pr^{*} and Ra^{*} are respectively the modified Prandtl and Rayleigh numbers for nanofluid

$$Pr^{*}=\frac{\mu_{nf}}{\mu_{f}}\frac{C_{pnf}}{C_{p_{f}}}\frac{k_{f}}{k_{nf}}Pr \tag{11}$$

$$Ra^{*}=\frac{(\rho\beta)_{nf}}{(\rho\beta)_{f}}\frac{k_{f}}{k_{nf}}\frac{(\rho C_{p})_{nf}}{(\rho C_{p})_{f}}\frac{\mu_{f}}{\mu_{nf}}Ra \tag{12}$$

Table 1
The non-dimensional boundary conditions

X=0	X=W	Y=0, H	X=X_1, X_2
θ=1	θ=0	$\frac{\partial \theta}{\partial Y}=0$	$\left(\frac{\partial \theta}{\partial X}\right)_{nf}=\frac{k_s}{k_{nf}}\left(\frac{\partial \theta}{\partial X}\right)_{solid}$
U=V=0	U=V=0	U=V=0	U=V=0

3. Thermo-physical properties of the nanofluid

3.1. At the ambient temperature

The density, the specific heat capacity and the thermal expansion coefficient of Al2O3–water nanofluid at the ambient temperature are summarized in Table 2.

Table 2
Thermo-physical properties of the nanofluid at the ambient temperature

Physical property	*Equation*	*Reference*
density	$\rho_{nf}=(1-\phi)\rho_f+\phi\rho_p$	[36]
heat capacitance	$(C_p)_{nf}=(1-\phi)(C_p)_f+\phi(C_p)_p$	[38]
ρ-weighted heat capacity	$(\rho C_p)_{nf}=(1-\phi)(\rho C_p)_f+\phi(\rho C_p)_p$	[39], [43]
ρ-weighted thermal expansion coefficient	$(\rho\beta)_{nf}=(1-\phi)(\rho\beta)_f+\phi(\rho\beta)_p$	[36]

The effective thermal diffusivity of the nanofluid is given by the following expression:

$$\alpha_{nf}=\frac{k_{nf}}{(\rho C_p)_{nf}} \tag{13}$$

3.2. Dependence on temperature

Based on the experimental data of Ho *et al.,* [44], Khanafer and Vafai [33] developed a new correlation for the density, the specific heat capacity and the thermal expansion coefficient of Al_2O_3–water nanofluid at different temperatures and nanoparticles volume fraction, which are grouped in Table 3.

Table 3
Thermo-physical properties of the nanofluid for various temperatures

Physical property	*Equation*
Density	$\rho_{nf}(T)=1001.064+2738.6191\times\phi-0.2095\times T$
Heat capacitance	$Cp_{nf}=\left(\frac{(1-\phi)\times Cp_f\times\rho_f+\phi\times\rho_p\times Cp_p}{\rho_{nf}(T)}\right)$
Thermal expansion coefficient	$\beta_{nf}(T)=\left(-0.479\times\phi+T\times9.3158\times10^{-3}-\frac{4.7211}{T^2}\right)\times10^{-3}$

4. Models of viscosity and thermal conductivity

4.1. At room temperature

Several models have been established for the nanofluid viscosity and hermal conductivity at room temperature. Tables 4 and 5 present some theoretical and measurement fitting models.

Table 4
Summary of viscosity models at room temperature

Theoretical models	*Experimental models*	*Remarks*
Brinkman model [18] $\mu_{nf}=\frac{\mu_f}{(1-\phi)^{2.5}}$	Khanafer and Vafai [33] $\mu_{nf}=\left(1+23.09\phi+1525.3\phi^2\right)\mu_f$	Fitting measurements of Pak and Cho [36] d_p=13nm, $0\le\phi\le 0.04$
Batchelor model [45] $\mu_{nf}=\left(1+2.5\phi+6.2\phi^2\right)\mu_f$	Maiga *et al.,* [46] $\mu_{nf}=\left(1+7.3\phi+123\phi^2\right)\mu_f$	Fitting measurements of Wang *et al.,* [47] d_p=28nm

Table 5
Summary of thermal conductivity models at room temperature

Theoretical model	*Experimental model*
Maxwell, Hamilton and Crosser model [15, 16] $k_{nf}=k_f\frac{k_p+2k_f-2\phi\left(k_f-k_p\right)}{k_p+2k_f+\phi\left(k_f-k_p\right)}$	Khanafer and Vafai [33] $\frac{k_{nf}}{k_f}=1+1.0112\phi+2.4375\phi\left(\frac{47}{d_p}\right)-0.0248\phi\left(\frac{k_p}{0.613}\right)$ $0\le\phi\le 0.04,\ 10°C\le T\le 40°C$

4.2. At various temperatures

By fitting the curve of the experimental data [32], [34-36] available in the literature Khanafer and Vafai [33] developed a new correlations for the effective viscosity of based Al_2O_3-water nanofluid. The models is valid for Al_2O_3-water nanofluid with temperatures between 20 and 70 °C, nanoparticles diameter between 13 and 131 nm and volume concentrations between 1% and 9%.

$$\mu_{nf}(T)=\mu_f\left(-0.4491+\frac{28.837}{T}+0.5740\times\phi-0.1634\times\phi^2+23.053\times\frac{\phi^2}{T^2}+0.0132\times\phi^3-2354.734\times\frac{\phi}{T^3}+23.498\frac{\phi^2}{d_p^2}-3.0185\frac{\phi^3}{d_p^2}\right) \quad (14)$$

The dynamic viscosity μ_f of pure water versus the temperature can be expressed as follow

$$\mu_f(T)=2.414\times10^{-5}\times10^{\frac{247.8}{T-140}} \quad (15)$$

The correlation corresponding to the relative thermal conductivity of the nanofluid is approximated by Khanafer and Vafai [33] based on experimental data.

$$\frac{k_{nf}(T)}{k_f(T)}=0.9843+0.398\times\phi^{0.7383}\times\left(\frac{1}{d_p}\right)^{0.2246}\times\left(\frac{\mu_{nf}(T)}{\mu_f(T)}\right)^{0.0235}-3.9517\times\frac{\phi}{T}+34.034\times\frac{\phi^2}{T^3}+32.509\times\frac{\phi}{T^2} \quad (16)$$

$11\,nm\le d_p\le 150\,nm,\ 20°C\le T\le 70°C$

5. Lattice Boltzmann Method

For the incompressible problems, LBM utilizes two distribution functions, *f* and *g*, for the flow and temperature fields, respectively [48].

For the flow field:

$$f_k\left(x+c_{k=0-8}\Delta t,t+\Delta t\right)-f_k\left(x,t\right)=\frac{1}{\tau_\upsilon}\left[f_k^{eq}\left(x,t\right)-f_k\left(x,t\right)\right]+\Delta t\ F_k \tag{17}$$

For the temperature field:

$$g_k\left(x+c_{k=0-8}\Delta t,t+\Delta t\right)-g_k\left(x,t\right)=\frac{1}{\tau_c}\left[g_k^{eq}\left(x,t\right)-g_k\left(x,t\right)\right] \tag{18}$$

τ_υ and τ_c are the relaxation time for the flow and temperature fields

F is an external force term

f_{eq} and g_{eq} are the local equilibrium distribution functions which are calculated with Eqs. 19 and 20 for flow and temperature fields, respectively.

$$f_k^{eq}=\rho\omega_k\left[1+3\frac{c_k.u_i}{c^2}+\frac{9\left(c_k.u_i\right)^2}{2c^4}-\frac{3{u_i}^2}{2c^2}\right] \tag{19}$$

$$g_k^{eq}=\omega_k\theta\left[1+3\frac{c_k.u_i}{c^2}\right] \tag{20}$$

D2Q9 model for flow and temperature is used in this work, thus the weighting factors and the discrete particle velocity vectors are calculated as follows:

$$\omega_{k=0}=\frac{4}{9},\omega_{k=1-4}=\frac{1}{9},\omega_{k=5-8}=\frac{1}{36} \tag{21}$$

The discrete velocities, c_i , for the D2Q9 (Figure 2) are defined as follows:

$$c_i=\begin{pmatrix}c_{ix}\\c_{iy}\end{pmatrix}=\begin{pmatrix}0&1&0&-1&0&1&-1&-1&1\\0&0&1&0&-1&1&1&-1&-1\end{pmatrix} \tag{22}$$

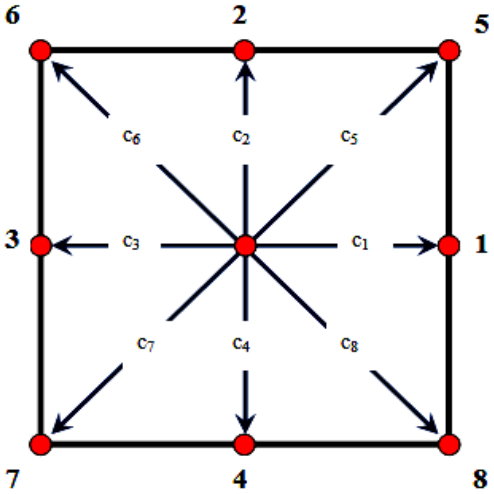

Fig. 2. The nine-speed square lattice of the D2Q9 model for the flow and temperature fields

The kinematic viscosity and the thermal diffusivity are then related to the relaxation times by:

$$\upsilon = \left[\tau_{\upsilon} - \frac{1}{2}\right] c_s^2 \Delta t \tag{23}$$

$$\alpha = \left[\tau_c - \frac{1}{2}\right] c_s^2 \Delta t \tag{24}$$

Where c_s is the lattice speed sound which is equal to $c_s = \frac{c}{\sqrt{3}}$

The macroscopic quantities can be calculated with the following formula:

Flow density: $\rho(x,t) = \sum_{k=0}^{8} f_k$ (25)

Momentum: $\rho(x,t)u_i(x,t) = \sum_{k=0}^{8} c_k f_k$ (26)

Temperature: $\theta(x,t) = \sum_{k=0}^{8} g_k$ (27)

5.1. Conjugate heat transfer formulation

At the fluid-solid interface, the temperature and heat flux are continuous, as described in the following equations

$$k_{nf}\left(\frac{\partial\theta}{\partial X}\right)_{nf} = k_s\left(\frac{\partial\theta}{\partial X}\right)_s \tag{28}$$

$$\left(\frac{\partial\theta}{\partial X}\right)_{nf} = k_r\left(\frac{\partial\theta}{\partial X}\right)_s \tag{29}$$

Where $k_r = \frac{k_s}{k_{nf}}$.

As a consequence, in the present model, the temperature and the heat flux at the interface can be kept continuous naturally. Solving the Eq. 29 for the temperature at the interface leads to:

At X=X_1

$$\theta(i,j) = \frac{\theta_{nf}(i-1,j) + k_r \times \theta_s(i+1,j)}{1+k_r} \tag{30}$$

At X=X_2

$$\theta(i,j) = \frac{k_r \times \theta_s(i-1,j) + \theta_{nf}(i+1,j)}{1+k_r} \tag{31}$$

6. Solution method

The viscosity and thermal diffusivity are calculated from the definition of these non-dimensional parameters

$$\upsilon_f = N \times Ma \times c_s \times \sqrt{\frac{Pr}{3 \times Ra}} \tag{32}$$

$$\alpha_f = \frac{\upsilon_f}{Pr}$$

where N is the number of lattices nodes in y-direction

In the present study, Mach number is fixed as 0.1. In order to ensure that the code is applicable in a near incompressible regime, the characteristic velocity must be small compared to the fluid speed of sound**.**

The Nusselt number *Nu* is the most important dimensionless parameters describing the convective heat transport. The local Nusselt number is expressed as:

$$Nu_l = \frac{hH}{k_f} \tag{33}$$

Where the heat transfer coefficient is computed from:

$$h = \frac{q_w}{T_h - T_c} \tag{34}$$

The thermal conductivity of the nanofluid is expressed as:

$$k_{nf} = -\frac{q_w}{\frac{\partial T}{\partial X}} \tag{35}$$

The local Nusselt number along the left wall can be calculating by substituting the Eqs. 34 and 35 into Eq. 33, and using the dimensionless quantities, can be written as:

$$Nu_l = -\frac{k_{nf}}{k_f}\left(\frac{\partial T}{\partial X}\right)_{X=0}$$

The average Nusselt number is obtained by integrating the local Nusselt number

$$\overline{Nu_l} = -\frac{1}{H}\int_0^H \frac{k_{nf}}{k_f}\left(\frac{\partial T}{\partial X}\right)_{X=0}$$

7. Grid independence test and code validation

In order to check the grid sensitivity and the code validation the models of Brinkman [18] and Hamilton and Crosser [16] for viscosity and the effective thermal conductivity respectively are used.

7.1. Grid independence test

In order to guarantee a grid independent solution, various grids (50^2, 100^2, 150^2, 200^2 and 250^2) were tested for the enclosure with partition filled with 4% of Al_2O_3-water. The results are shown in Figure 3 by the vertical velocity profile. According to this figure, 200×200 lattices number is chosen as the final independent lattice numbers for all Rayleigh numbers.

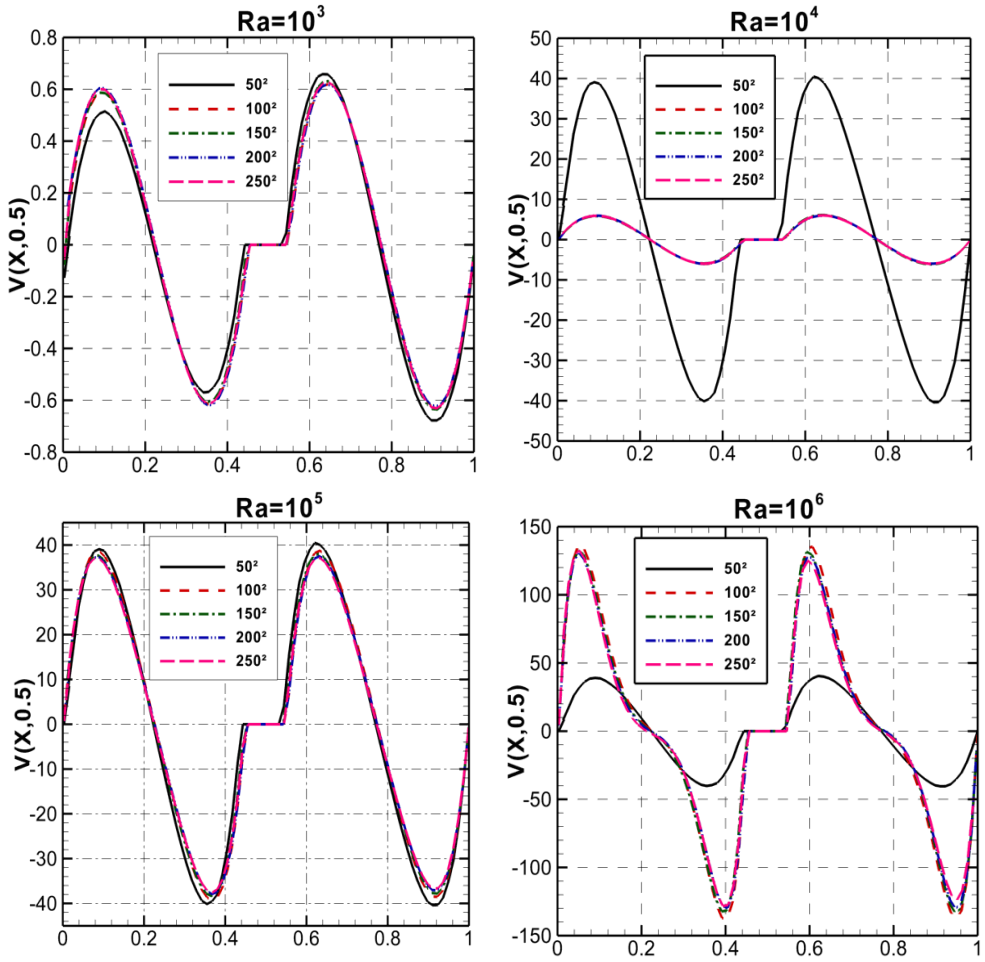

Fig. 3. Grid sensitivity check: Vertical velocity profile U (X, 0.5) for different mesh sizes at different Rayleigh numbers (4% Al_2O_3/water nanofluid)**.**

7.2. Code validation

The validation of the present numerical work is performed by comparing the results of the average Nusselt number obtained by the present code for different values of Rayleigh number with results available in the literature for the two test cases. At the first, the comparison presented in Table 6 for natural convection in an enclosure filled with air and water (Pr=0.71 and 5.828 respectively) shows that there is very good agreement between the results of the present LBM method and results of [[20], [49]] based on the LBM method and PDQ method respectively. Our results are also validate based to an experimental study realized by Bairi [50]. The results show a max deviation about 6.59% for Ra=10^6.

The second, it concerns natural convection in an enclosure filled with Al_2O_3-water nanofluid, the results obtained by the present code for different Rayleigh number and for different solid volume fraction are compared with those performed by [20] based on the LBM method (Table 7). From this table we noted that the solutions are in excellent agreement.

The present model correspond to a differentially heated cavity with conjugate heat transfer was validate by comparison to FE COMSOL [51] results for k_r=6.22, Pr=0.71, δ=0.1 and Ra=10^5. Figure 4 illustrates the temperature profiles and the local Nusselt number of the active hot wall. The results show an excellent agreement.

Table 6
Comparison of the present results for a differentially heated cavity at different Rayleigh numbers with results of Refs [20], [49] and [50].

		Air					Water		
		Present	Ref [20]	Ref [49]	Ref [50]		Present	Ref [20]	Ref [49]
Method		LBM	LBM	PDQ	Exp.	Max devi.	LBM	LBM	PDQ
Ra	10^3	1.127	1.126	1.118	1.112	1.33	1.126	1.128	-
	10^4	2.253	2.252	2.243	2.168	3.77	2.284	2.286	2.274
	10^5	4.522	4.514	4.519	4.228	6.5	4.732	4.729	4.722
	10^6	8.825	8.752	8.799	8.243	6.59	9.299	9.173	9.230

Table 7
Comparison of the present results for a square cavity filled with Al_2O_3-water nanofluid at different Rayleigh numbers with results of Ref [20].

Ra	Volume fraction (φ (%))	Ref **[20]**	Present study	Error (%)
10^3	1	1.16	1.16	0
	2	1.19	1.19	0
	3	1.22	1.22	0
	4	1.26	1.26	0
10^4	1	2.35	2.34	0.4
	2	2.41	2.41	0
	3	2.48	2.48	0
	4	2.55	2.55	0
10^5	1	4.86	4.85	0.2
	2	5.00	4.99	0.2
	3	5.14	5.14	0
	4	5.28	5.28	0
10^6	1	9.43	9.57	1.48
	2	9.69	9.84	1.54
	3	9.96	10.12	1.6
	4	10.24	10.40	1.56

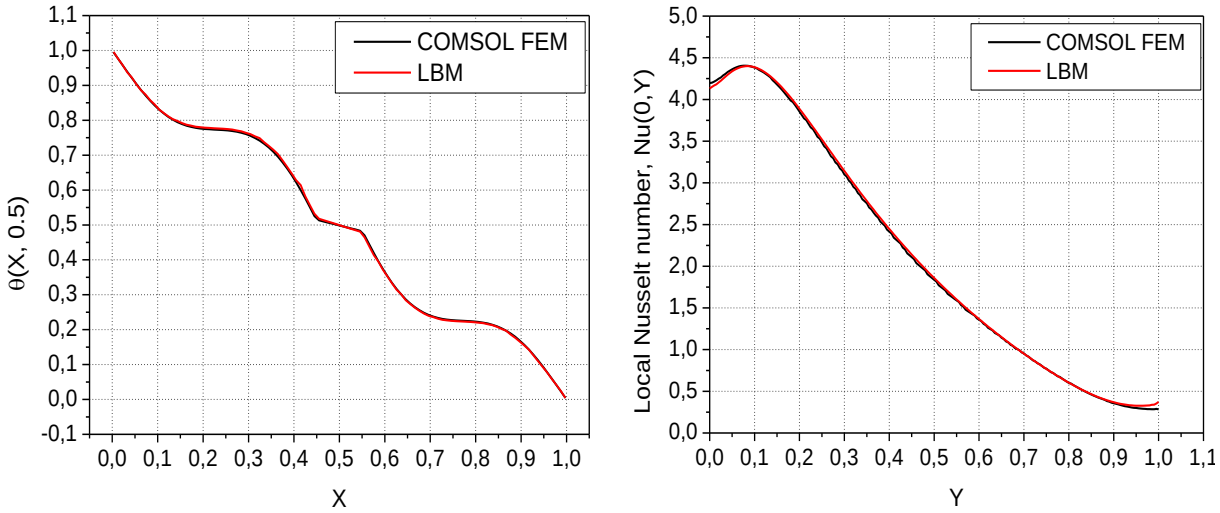

Fig. 4. Temperature profile θ(X, 0.5) (a) and the Local Nusselt number (b) compared with those obtained by COMSOL.

8. Results

In the present investigation, the conjugate natural convention heat transfer phenomenon in a square cavity containing an exchanger is studied using lattice Boltzmann method based on experimental correlations. The divided cavity is filled with water based Al_2O_3 nanofluid. In this study, the effects of several parameters such as volume fraction of nanoparticles ($1\% \leq \varphi \leq 4\%$), Rayleigh number ($10^3 \leq Ra \leq 10^6$), temperature variation and the effect of particles size have been examinated. the Prandtl number is fixed at Pr = 6.2.

8.1. Simulation at room temperature

Figure 5 shows a comparison of the relative dynamic viscosity of water based Al_2O_3 nanofluid at room temperature. The viscosity models at room temperature are summarized in Table 4. As seen from the figure that the dynamic viscosity increase by adding nanoparticles into the basic fluid.

Based on the experimental correlation proposed by Khanafer and Vafai [33], we find from the Figure 5 that the relative dynamic viscosity of Al_2O_3-water nanofluid is 4.36408 for 4% nanoparticles concentration. For the same concentration of nanoparticles, the Brinkman model [18] gives a relative viscosity of only 1.10744. The deviation is about 74.62%. It is found clearly that the relative dynamic viscosity of Al_2O_3-water nanofluid is largely underestimated by theoretical models especially at high concentrations. The augmentation in relative viscosity corresponding to the Khanafer and Vafai model is more important than the augmentation in relative viscosity estimated by the Brinkman model when the volume fraction of the nanofluid increases from 0 to 4%.

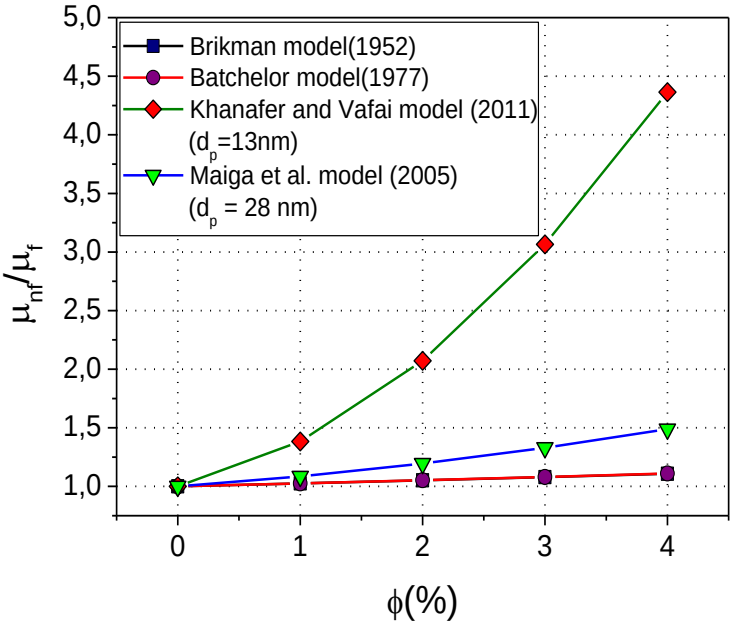

Fig. 5. Comparison of the experimental models used in this study to theoretical models (Brinkman and Batchelor) for Al_2O_3-water corresponding to the viscosity for different volume fraction

Several experimental and theoretical studies in the literature have reported to estimate the thermal conductivity of nanofluids at room temperature (Table 5). Figure 6 show a comparison of the effective thermal conductivity measurements estimated by the experimental model proposed by Khanafer and Vafai [33] to the theoretical model of Hamilton and Crosser [16] at ambient temperature for Al_2O_3–water at various volume concentrations. For 4% nanoparticles concentration, the relative thermal conductivity corresponding to the Khanafer and Vafai model is about 1.32822. Furthermore, for the theoretical model, at the same nanoparticles concentration the estimated relative thermal conductivity is about 1.1192. The deviation of the experimental model proposed by Khanafer and Vafai [33] to the theoretical one is 15.73%. As the nanoparticles concentration increase for 0 to 4%, we remark that the relative thermal conductivity of the water based Al_2O_3 nanofluid estimated by the experimental model undergoes an augmentation of 24.71%. For the theoretical model the enhancement of the relative thermal conductivity is about 10.65%.

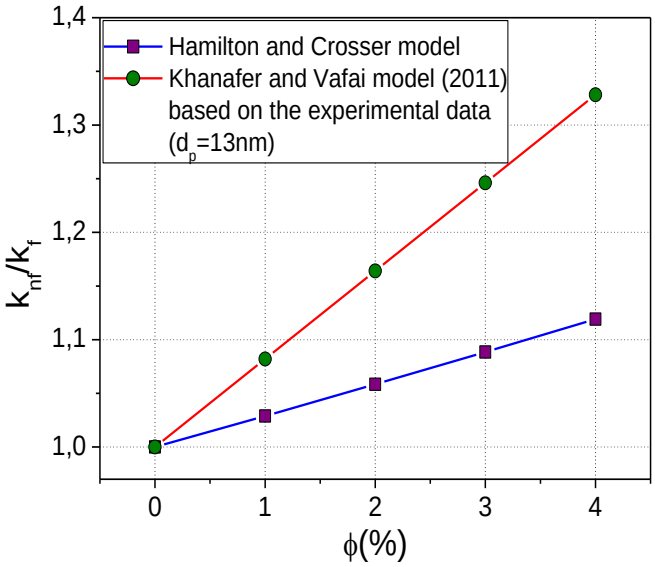

Fig. 6. Comparison of the experimental model proposed by Khanafer and Vafai to theoretical model for Al_2O_3-water corresponding to the thermal conductivity for different volume fraction

Figure 7 shows the variation of the Nusselt number versus the nanoparticles concentration of Al2O3 in the base fluid using the model proposed by Khanafer and Vafai [33] for the dynamic viscosity (Eq. 23) and thermal conductivity (Eq. 28). The results estimated by experimental model are compared to the theoretical model of Brinkman [18] (Eq. 21). As seen from the figure that the experimental model of Khanafer and Vafai lead to decrease in heat transfer when the nanoparticles concentration increases. This decrease is more pronounced for high Rayleigh number. More precisely, for Ra=103, 104, 105, 106, the average Nusselt number decreases respectively by 0%, 2.53%, 33.22% and 32. 01%. When we use the model of Brinkman the heat transfer is always improved.

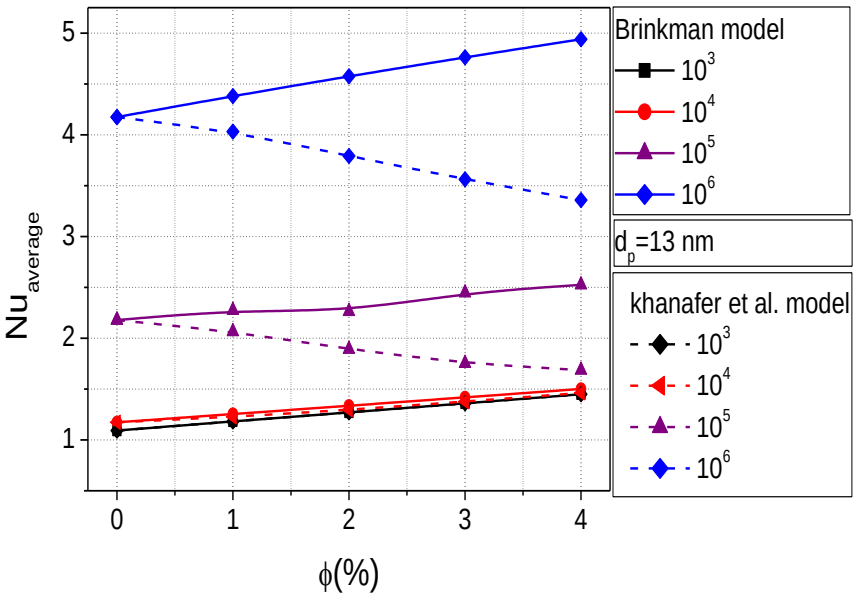

Fig. 7. The average Nusselt number as a function of solid volume fraction of Al_2O_3 for different Rayleigh numbers

The Nusselt number is the ratio of convection heat transfer to conduction heat transfer. Besides, the addition of nanoparticles into the base fluid increases the thermal conductivity of the nanofluid and then increases heat transfer, especially by conduction from the hot wall to flow and the conduction mode of heat transfer becomes dominant, but also increases its viscosity and then slow the flow motion leading to a decrease in heat transfer by convection inside the cavity. Who is the responsible to the decrease in heat transfer inside the partitioned cavity? Answer this question allows us to predict the behavior of the Nusselt number. As seen from the previous figures that the augmentation in relative viscosity is more important than the augmentation in the relative thermal conductivity. Besides, the increase in relative thermal conductivity is dominated by the increase in nanofluid viscosity. As a consequence, this decrease in Nusselt number is generated by the convective effects.

Figure 8 illustrates the vertical velocity profile V(X, 0.5) for two models of viscosity at different Rayleigh numbers. As seen from the figure the absolute value of the velocity depends strongly of the used models for viscosity. The use of the model based on the experimental correlations lead to reduce the amplitude of the velocity with 64.70% for $Ra=10^5$, for $Ra=10^6$ the decrease is about 50%. Because of the high deviation between the two models, we think that the model based on the experimental correlations is more credible than the Brinkman model which is based on theoretical considerations.

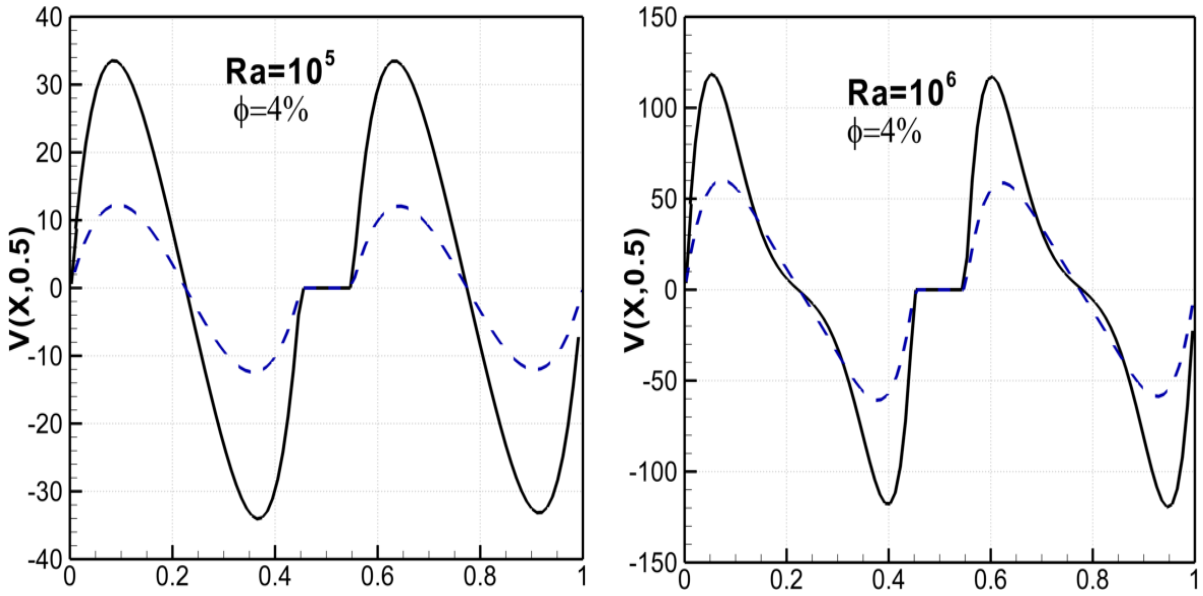

Fig. 8. Vertical velocity profile V(X, 0.5) for two models of viscosity (solid line correspond to the Brinkman model), (dashed line correspond to Khanafer and Vafai model) at different Rayleigh numbers

Figure 9 shows the variation of the viscosity of nanofluid as a function of temperature for different volume fraction. We observe from this figure, as the temperature increase the viscosity of the base fluid decreases. The particles get rid of the effect of viscous forces, which leads to a decrease in the viscosity of the nanofluid for each concentration of the nanofluid. For example, at 4% particles concentration, it is found that the viscosity of water based Al_2O_3 nanofluid decrease by 52.66% when the temperature ranges between 20°C and 40°C.

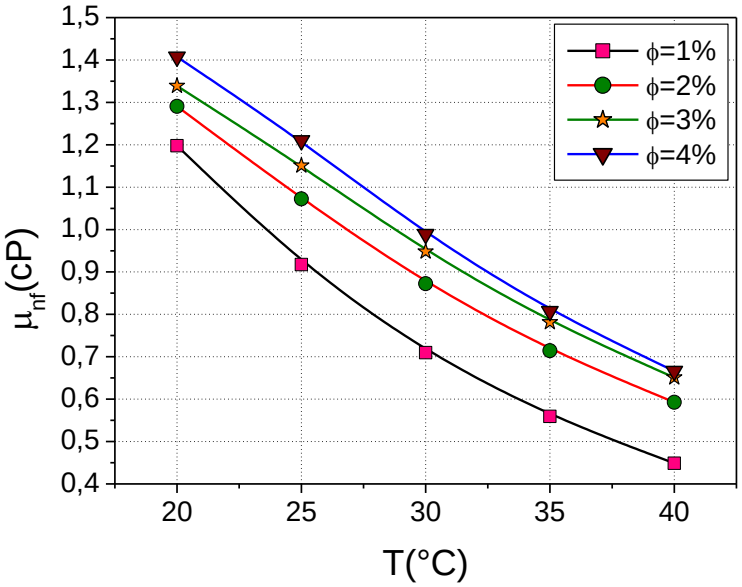

Fig. 9. Variation of the viscosity of Al_2O_3-water nanofluid versus temperature for different concentrations of nanofluid

8.2. Effect of temperature variation

Figure 10 illustrates the influence of temperature on the relative thermal conductivity for various nanofluid concentrations. As the temperature increase the thermal conductivity ratio increase according to quasi linear variation. The main cause of improving of thermal conductivity due to the temperature rising may be described by the augmentation of interactions between the nanoparticles and Brownian motion. Moreover, at higher particles concentration, the ratio of surface to volume and collisions between particles increase which lead to the enhancement of the relative thermal conductivity. It may of. At φ=4%, the rate of augmentation of the relative thermal conductivity is about 7.5% when temperature range between 20°C and 40°C.

For ϕ=1%:

$$\overline{Nu} = 2{,}83637 + 0{,}05775 \times T - 1{,}62857 \times T^2 \times 10^{-4}$$

For ϕ=4%:

$$\overline{Nu} = 3{,}38603 + 0{,}01235 \times T - 5{,}02857 \times T^2 \times 10^{-4}$$

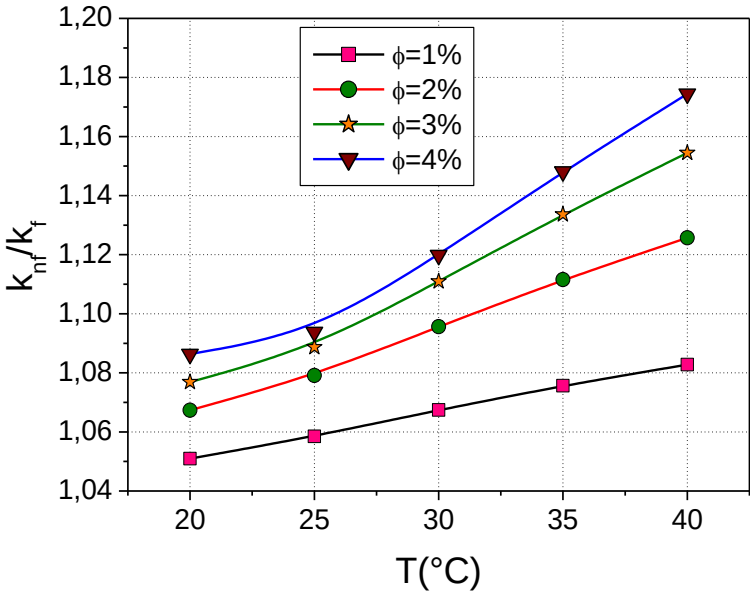

Fig. 10. Variation of the relative thermal conductivity of Al_2O_3-water nanofluid versus temperature for different concentration of nanofluid

Figure 11 illustrate the variation of the mean heat transfer as a function of temperature and for different nanoparticles volume fraction. We observe from the figure that the average Nusselt number increase linearly with increasing temperature indicating the improvement of heat transfer performance. In order to predict the average Nusselt number of Al_2O_3-water nanofluid, a correlation is presented by a second order polynomial fit. This correlation is a function of the nanofluid temperature for different solid volume fraction.

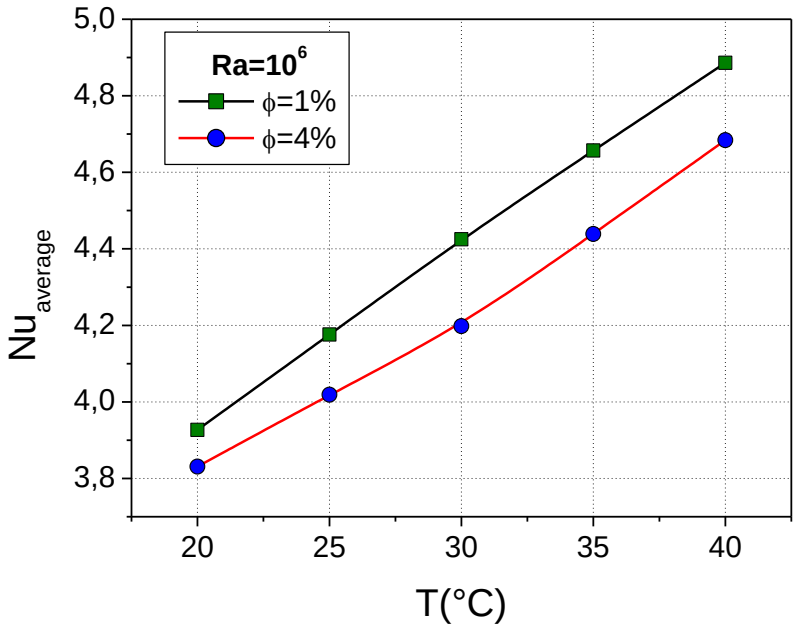

Fig. 11. Variation of the average Nusselt number of Al_2O_3-water nanofluid as a function temperature for different concentrations of nanofluid

Figure 12 displays the variation local Nusselt number along the hot wall for different temperatures and for different nanoparticles volume fraction. It is clear that the local Nusselt

number increases with increasing in the temperature for each concentration of the mixture. As discussed above, the viscosity of Al_2O_3-water mixture decreases considerably with increasing temperature. In terms of solid volume fraction, the local Nusselt number of nanofluid decreases with the addition of nanoparticles. This decrease respect to the concentration of Al_2O_3 in the base fluid confirms the behavior of the average Nusselt number discussed above. The local Nusselt takes on higher values around Y=0 due to the higher temperature difference between the wall and the fluid.

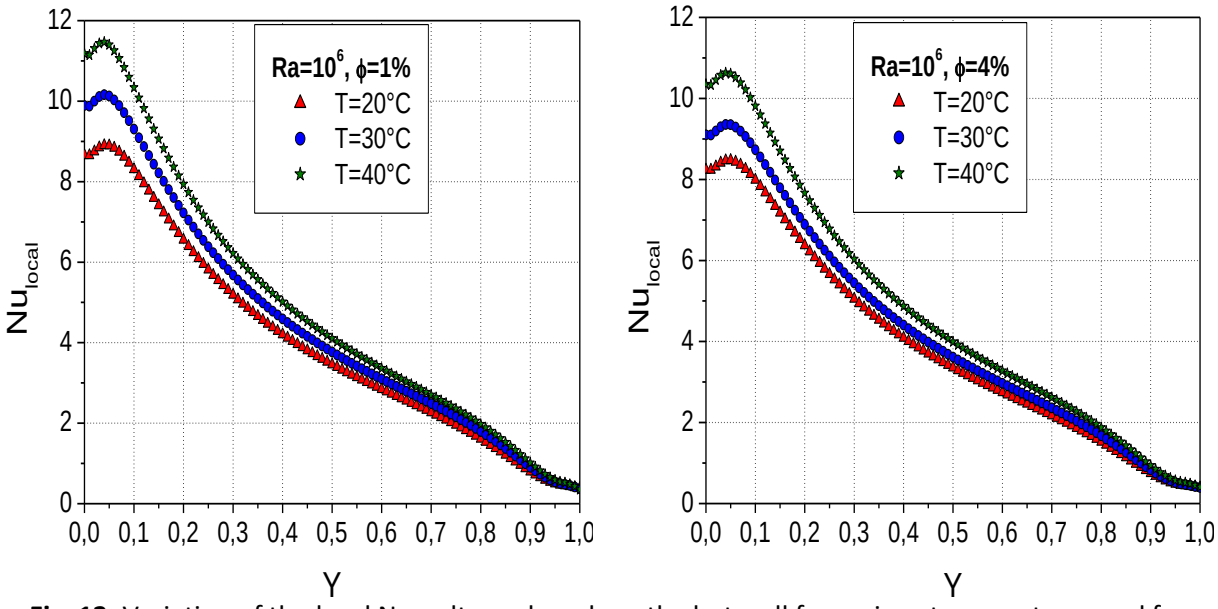

Fig. 12. Variation of the local Nusselt number along the hot wall for various temperatures and for different nanoparticles volume fraction

Figure 13 displays the vertical velocity profile at the midplan for various temperatures and for different concentration of Al_2O_3 in the base fluid. It is seen that the amplitude of the velocity increase with increasing the temperature. Besides, the decrease in viscosity and the increase of the thermal conductivity lead to reduce the viscous forces and the flow becomes freer. This is a favorable situation to improve the heat transfer. In terms of solid volume fraction, we observe that the amplitude of the velocity decrease with the addition of Al_2O_3 nanosuspension into the base fluid.

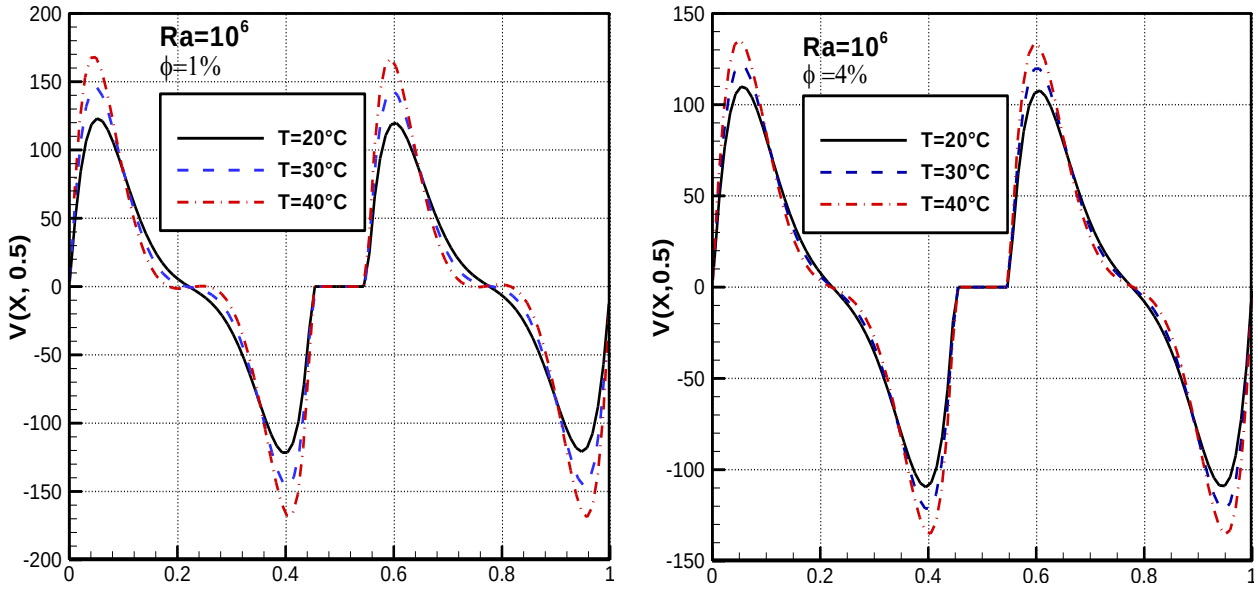

Fig. 13. Vertical velocity profile V(X, 0.5) for various temperatures and for different nanoparticles volume fraction

8.3. Effect of nanoparticles diameter size

Figure 14 illustrates the influence of nanoparticles diameter on the viscosity of nanofluid for different temperature. By analyzing this figure, we observe that the viscosity decrease strongly when the nanoparticles diameter ranging from 15nm to 45nm. As seen that the viscosity remains constant at the interval 45 to 120. However, at low nanoparticles diameter the surface area between the nanoparticles increases. Besides, the viscous effect relative to the base fluid increase and leads to the increase in the viscosity of nanofluid.

Figure 15 depicts the influence of nanoparticles diameter on the relative thermal conductivity of nanofluid for different temperature. As seen from this figure that the effective thermal conductivity of nanofluid decreases when the nanoparticles diameter increases. Besides, by increasing the nanoparticles diameter the spaces inter nanoparticles decrease and lead to decreases in thermal conductivity. In addition, when the surface between the nanosuspensions increase the interfacial layers which is the first responsible of the increase in the thermal conductivity increase.

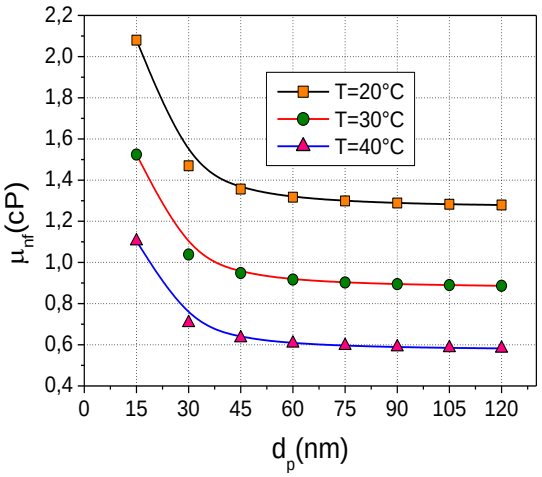

Fig. 14. Variation of the dynamic viscosity of Al_2O_3-water nanofluid versus nanoparticles diameter for various temperatures

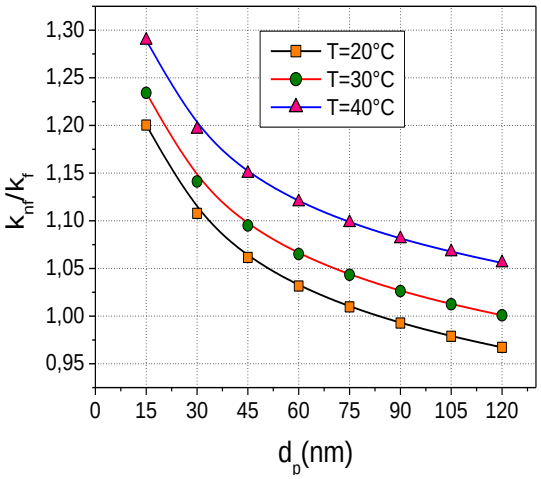

Fig. 15. Thermal conductivity ratio of Al2O3-water nanofluid versus nanoparticles diameter for various temperatures

The effect of nanoparticles diameter of Al_2O_3 on the average Nusselt number at is depicted in Figure 16. By analyzing the previous figure, we find that the Nusselt number increases considerably with increasing the diameter size of Al_2O_3 nanoparticles when d_p is lower than 30 nm. The Nusselt number achieved a maximum value in the range of 30-37.5 nm. It is clear from the previous figure that an increase in the nanoparticles diameter leads to reduction of the heat transfer rate on the hot wall. This behavior is observed when d_p is higher than 45 nm. The size of the nanoparticles has a considerable effect on the viscosity and thermal conductivity of water based Al_2O_3 nanoparticles. Consequently, he affects the flow and heat transfer characteristics. The enhancement in Nusselt number when d_p is lower than 30 nm is due to the decrease of viscous nanofluid. By increasing the size of the nanoparticles the heat transfer becomes generated by the conductive mode. In order to obtain a good performance in heat transfer it is better to use smaller nanoparticles diameter.

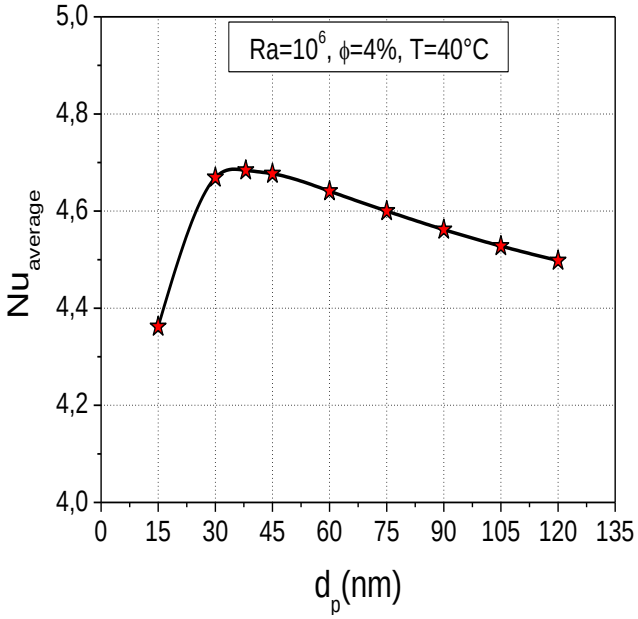

Fig. 16. Variation of the average Nusselt number of Al_2O_3-water nanofluid as a function of diameter size of nanoparticles

Figure 17 illustrates the dependence of the local Nusselt number along the hot wall on the size of nanoparticles. As seen from the figure that the local heat transfers is maximal when the nanoparticles diameters range from 38 to 75nm. For d_p less than 38 and lower than 75 the local Nusselt number decrease. Besides, the performance of the heat transfer at the active walls is detected at the interval [38nm; 75nm].

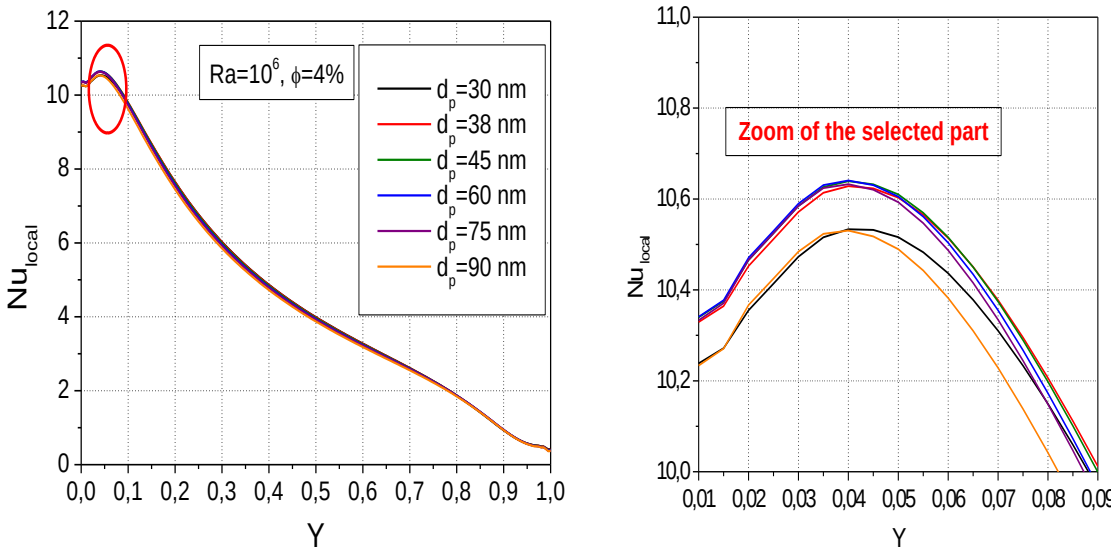

Fig. 17. Variation of the local Nusselt number along the hot wall of Al_2O_3-water nanofluid as a function of nanoparticles diameter size.

Figure 18 shows the dependence of vertical velocity profile V(X, 0.5) on nanoparticles size. As seen from the figure that the maximum and minimum values of velocity profiles are clearly affected by the size of particles diffused into the base fluid. As the diameter sizes increases the velocity fields present a symmetrical behavior for each part of the cavity. In addition, it is clear that when the size of particles increases the location of V_{max} moves to the wall and the solid partition.

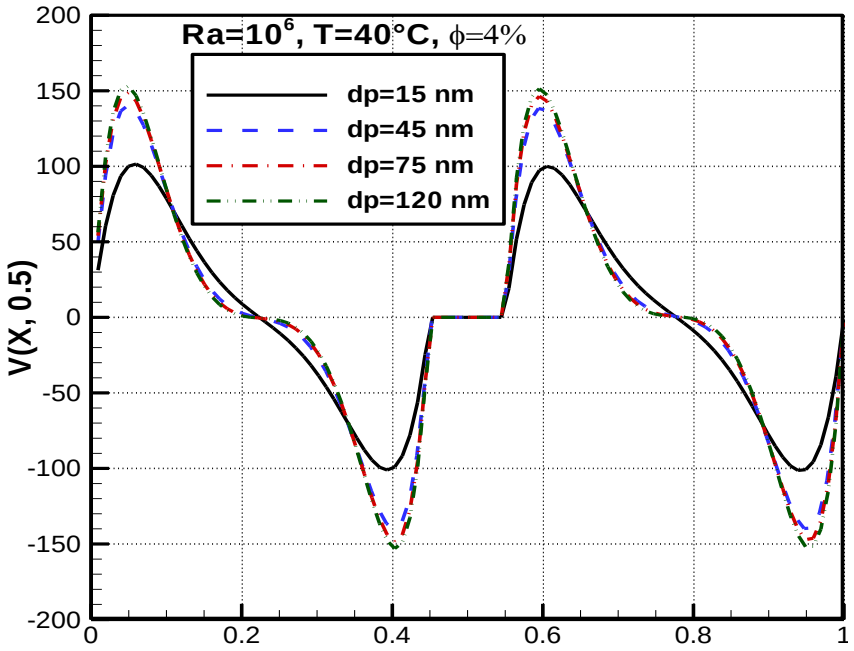

Fig. 18. Vertical velocity profile V(X, 0.5) for various diameter sizes of nanoparticles.

9. Important outcomes and conclusion

In this paper, a numerical investigation of conjugate natural convection flow and heat transfer in a partitioned cavity filled with Al_2O_3-water nanofluid based on experimental correlationshas been performed. The problem governing equations are solved using the lattice Boltzmann method. The

effects of the problem monitoring parameters on the flow dynamics and heat transfer are analyzed. The drawn conclusions may be summarized as follows:

a) At ambient temperature
   - The theoretical models underestimate the dynamic viscosity and thermal conductivity of nanofluid at high value of concentration of Al_2O_3.
   - The heat transfer decrease as the volume fraction increase.
   - The dynamic viscosity plays an important role to generate the heat transfer inside the partitioned cavity.

b) Above ambient temperature
   - The temperature is an important factor which affects the dynamic viscosity and thermal conductivity.
   - The enhancement is developed as the temperature increase.
   - The temperature affects strongly the dynamic of the flow.

c) Nanoparticlessize effect
   - Both dynamic viscosity and thermal conductivity decrease by increasing the nanoparticles size.
   - The size of the nanoparticles affects strongly the mean heat transferand the convective behavior.

Besides, it has been shown that the Lattice Boltzmann method is a powerful approach for investigating heat and fluid flow problems in multiphases media as well as for its simplicity of coding and its reasonable convergence CPU time in such stationary problems. In the following steps MHD effects in micro-geometries will be accounted for as an issue of important interest.

References

[1] Frisch, Uriel, Brosl Hasslacher, and Yves Pomeau. "Lattice-gas automata for the Navier-Stokes equation."*Physical review letters* 56, no. 14 (1986): 1505.

[2] Ismail, A., L. Jahanshaloo, and A. Fazeli. "Lagrangian grid LBM to predict solid particles' dynamics immersed in fluid in a cavity." *J. Adv. Res. Fluid Mech. Therm. Sci.* 3, no. 1 (2014): 17-26..

[3] S. Chol and J. Estman, "Enhancing thermal conductivity of fluids with nanoparticles," ASME-Publications-Fed, vol. 231, pp. 99-106, 1995.

[4] Sidik, NA Che, and A. Safdari. "Modelling of convective heat transfer of nanofluid in inversed L-shaped cavities." *J. Adv. Res. Fluid Mech. Therm. Sci.* 21, no. 1 (2016): 1-16..

[5] Safaei, Mohammad Reza, Marjan Gooarzi, Omid Ali Akbari, Mostafa Safdari Shadloo, and Mahidzal Dahari. "Performance evaluation of nanofluids in an inclined ribbed microchannel for electronic cooling applications." In *Electronics cooling. IntechOpen*, 2016.

[6] Tsai, C. Y., H. T. Chien, P. P. Ding, B. Chan, T. Y. Luh, and P. H. Chen. "Effect of structural character of gold nanoparticles in nanofluid on heat pipe thermal performance." *Materials Letters* 58, no. 9 (2004): 1461-1465.

[7] Jajja, Saad Ayub, Wajahat Ali, and Hafiz Muhammad Ali. "Multiwalled carbon nanotube nanofluid for thermal management of high heat generating computer processor." *Heat Transfer—Asian Research* 43, no. 7 (2014): 653-666.

[8] Siddiqui, Aysha Maryam, Waqas Arshad, Hafiz Muhammad Ali, Muzaffar Ali, and Muhammad Ali Nasir. "EVALUATION OF NANOFLUIDS PERFORMANCE FOR SIMULATED MICROPROCESSOR." *Thermal Science* 21, no. 5 (2017).

[9] Ali, Hafiz Muhammad, and Waqas Arshad. "Thermal performance investigation of staggered and inline pin fin heat sinks using water based rutile and anatase TiO2 nanofluids." *Energy conversion and management* 106 (2015): 793-803.

[10] Tzeng, S-C., C-W. Lin, and K. D. Huang. "Heat transfer enhancement of nanofluids in rotary blade coupling of four-wheel-drive vehicles." *Acta Mechanica* 179, no. 1-2 (2005): 11-23.
[11] Ali, Hafiz Muhammad, Hassan Ali, Hassan Liaquat, Hafiz Talha Bin Maqsood, and Malik Ahmed Nadir. "Experimental investigation of convective heat transfer augmentation for car radiator using ZnO–water nanofluids." *Energy* 84 (2015): 317-324.
[12] Ali, H. M., M. D. Azhar, M. Saleem, Q. S. Saeed, and A. Saieed. "Water based Mgo nanofluids for thermal management of car radiator." *Journal of Thermal Science* 19, no. 6 (2015).
[13] Jordan, Andreas, Regina Scholz, Peter Wust, Horst Fähling, and Roland Felix. "Magnetic fluid hyperthermia (MFH): Cancer treatment with AC magnetic field induced excitation of biocompatible superparamagnetic nanoparticles." *Journal of Magnetism and Magnetic materials* 201, no. 1-3 (1999): 413-419.
[14] Sajid, Muhammad Usman, and Hafiz Muhammad Ali. "Recent advances in application of nanofluids in heat transfer devices: A critical review." *Renewable and Sustainable Energy Reviews* 103 (2019): 556-592.
[15] Maxwell, James Clerk. "A Treatise on Electricity and Magnetism, 1873, 3rd." (1954).
[16] Hamilton, R. L, and O. K. Crosser. "Thermal conductivity of heterogeneous two-component systems." *Industrial & Engineering chemistry fundamentals* 1, no. 3 (1962): 187-191.
[17] Davis, R. H. "The effective thermal conductivity of a composite material with spherical inclusions." *International Journal of Thermophysics* 7, no. 3 (1986): 609-620.
[18] Brinkman, H. C. "The viscosity of concentrated suspensions and solutions." *The Journal of Chemical Physics* 20, no. 4 (1952): 571-571.
[19] Jahanshahi, M., S. F. Hosseinizadeh, M. Alipanah, A. Dehghani, and G. R. Vakilinejad. "Numerical simulation of free convection based on experimental measured conductivity in a square cavity using Water/SiO2 nanofluid." *International communications in heat and mass transfer* 37, no. 6 (2010): 687-694.
[20] Lai, Feng-Hsiang, and Yue-Tzu Yang. "Lattice Boltzmann simulation of natural convection heat transfer of Al2O3/water nanofluids in a square enclosure." *International journal of thermal sciences* 50, no. 10 (2011): 1930-1941.
[21] Kefayati, GH R. "Lattice Boltzmann simulation of natural convection in nanofluid-filled 2D long enclosures at presence of magnetic field." *Theoretical and Computational Fluid Dynamics* 27, no. 6 (2013): 865-883.
[22] Selvan, Muthtamil. "Mixed convection in a lid-driven cavity utilizing nanofluids." *CFD Letters* 2, no. 4 (2011): 163-175.
[23] Snoussi, L., R. Chouikh, N. Ouerfelli, and A. Guizani. "Numerical simulation of heat transfer enhancement for natural convection in a cubical enclosure filled with Al2O3/water and Ag/water nanofluids." *Physics and Chemistry of Liquids* 54, no. 6 (2016): 703-716.
[24] Sheikholeslami, M., M. Gorji-Bandpy, S. M. Seyyedi, D. D. Ganji, Houman B. Rokni, and Soheil Soleimani. "Application of LBM in simulation of natural convection in a nanofluid filled square cavity with curve boundaries." *Powder Technology* 247 (2013): 87-94..
[25] Bararnia, H., K. Hooman, and D. D. Ganji. "Natural convection in a nanofluids-filled portioned cavity: the lattice-Boltzmann method." *Numerical Heat Transfer, Part A: Applications* 59, no. 6 (2011): 487-502.
[26] Zahan, Ishrat. "Effect of conjugate heat transfer on flow of nanofluid in an enclosure with heat conducting vertical wall and uniform heat flux." (2017).
[27] Zahan, Ishrat, and M. A. Alim. "Effects of Rayleigh number and wall conductivity on conjugate natural convection of nanofluid in a heat conducting rectangular vertical walled enclosure." In *AIP Conference Proceedings,* vol. 1980, no. 1, p. 050017. AIP Publishing, 2018.
[28] Ho, Ching-Jenq, M. W. Chen, and Z. W. Li. "Numerical simulation of natural convection of nanofluid in a square enclosure: effects due to uncertainties of viscosity and thermal conductivity." *International Journal of Heat and Mass Transfer* 51, no. 17-18 (2008): 4506-4516.

[29] Jalali, Houda, and Hassan Abbassi. "Numerical Investigation of Heat Transfer by Al 2 O 3–Water Nanofluid in Square Cavity." In *International Conference Design and Modeling of Mechanical Systems,* pp. 1129-1138. Springer, Cham, 2017.
[30] Alawi, Omer A., Nor Azwadi Che Sidik, Hong Wei Xian, Tung Hao Kean, and S. N. Kazi. "Thermal conductivity and viscosity models of metallic oxides nanofluids." *International Journal of Heat and Mass Transfer* 116 (2018): 1314-1325.
[31] Etaig, Saleh, Reaz Hasan, and Noel Perera. "Investigation of a new effective viscosity model for nanofluids." *Procedia Engineering* 157 (2016): 404-413.
[32] Nguyen, C. T., F. Desgranges, Gilles Roy, Nicolas Galanis, Thierry Maré, S. Boucher, and H. Angue Mintsa. "Temperature and particle-size dependent viscosity data for water-based nanofluids–hysteresis phenomenon." *International Journal of Heat and Fluid Flow* 28, no. 6 (2007): 1492-1506.
[33] Khanafer, Khalil, and Kambiz Vafai. "A critical synthesis of thermophysical characteristics of nanofluids." *International journal of heat and mass transfer* 54, no. 19-20 (2011): 4410-4428.
[34] Anoop, K. B., T. Sundararajan, and Sarit K. Das. "Effect of particle size on the convective heat transfer in nanofluid in the developing region." *International journal of heat and mass transfer* 52, no. 9-10 (2009): 2189-2195.
[35] Putra, Nandy, Wilfried Roetzel, and Sarit K. Das. "Natural convection of nano-fluids." *Heat and mass transfer* 39, no. 8-9 (2003): 775-784.
[36] Pak, Bock Choon, and Young I. Cho. "Hydrodynamic and heat transfer study of dispersed fluids with submicron metallic oxide particles." *Experimental Heat Transfer an International Journal* 11, no. 2 (1998): 151-170.
[37] Corcione, Massimo. "Empirical correlating equations for predicting the effective thermal conductivity and dynamic viscosity of nanofluids." *Energy Conversion and Management* 52, no. 1 (2011): 789-793.
[38] Sekhar, Y. Raja, and K. V. Sharma. "Study of viscosity and specific heat capacity characteristics of water-based Al2O3 nanofluids at low particle concentrations." *Journal of experimental Nanoscience* 10, no. 2 (2015): 86-102.
[39] Kulkarni, Devdatta P., Ravikanth S. Vajjha, Debendra K. Das, and Daniel Oliva. "Application of aluminum oxide nanofluids in diesel electric generator as jacket water coolant." *Applied Thermal Engineering* 28, no. 14-15 (2008): 1774-1781.
[40] Murshed, SM Sohel. "Simultaneous measurement of thermal conductivity, thermal diffusivity, and specific heat of nanofluids." *Heat Transfer Engineering* 33, no. 8 (2012): 722-731.
[41] Zhou, Sheng-Qi, and Rui Ni. "Measurement of the specific heat capacity of water-based Al 2 O 3 nanofluid." *Applied Physics Letters* 92, no. 9 (2008): 093123.
[42] O'Hanley, Harry, Jacopo Buongiorno, Thomas McKrell, and Lin-wen Hu. "Measurement and model validation of nanofluid specific heat capacity with differential scanning calorimetry." *Advances in Mechanical Engineering* 4 (2012): 181079.
[43] Palm, Samy Joseph, Gilles Roy, and Cong Tam Nguyen. "Heat transfer enhancement with the use of nanofluids in radial flow cooling systems considering temperature-dependent properties." *Applied thermal engineering* 26, no. 17-18 (2006): 2209-2218.
[44] Ho, C. J., W. K. Liu, Y. S. Chang, and C. C. Lin. "Natural convection heat transfer of alumina-water nanofluid in vertical square enclosures: an experimental study." *International Journal of Thermal Sciences* 49, no. 8 (2010): 1345-1353.
[45] Batchelor, G. K. "The effect of Brownian motion on the bulk stress in a suspension of spherical particles." *Journal of fluid mechanics* 83, no. 1 (1977): 97-117.
[46] Maiga, Sidi El Becaye, Samy Joseph Palm, Cong Tam Nguyen, Gilles Roy, and Nicolas Galanis. "Heat transfer enhancement by using nanofluids in forced convection flows." *International journal of heat and fluid flow* 26, no. 4 (2005): 530-546.
[47] Wang, Xinwei, Xianfan Xu, and Stephen U. S. Choi. "Thermal conductivity of nanoparticle-fluid mixture." *Journal of thermophysics and heat transfer* 13, no. 4 (1999): 474-480.

[48] Mohamad, A. A., and A. Kuzmin. "A critical evaluation of force term in lattice Boltzmann method, natural convection problem." *International Journal of Heat and Mass Transfer* 53, no. 5-6 (2010): 990-996.
[49] Kahveci, Kamil. "Buoyancy driven heat transfer of nanofluids in a tilted enclosure." *Journal of Heat Transfer* 132, no. 6 (2010): 062501.
[50] Bairi, A. "Nusselt–Rayleigh correlations for design of industrial elements: Experimental and numerical investigation of natural convection in tilted square air filled enclosures." *Energy conversion and management* 49, no. 4 (2008): 771-782.
[51] COMSOL Multiphysics Reference Manual, version 4.3, COMSOL, Inc, www.comsol.com.